IEEJ TRANSACTIONS ON ELECTRICAL AND ELECTRONIC ENGINEERING
IEEJ Trans 2017; **12**: 744–752
Published online in Wiley Online Library (wileyonlinelibrary.com). DOI:10.1002/tee.22461

Paper

Permanent Magnet Synchronous Motor Torque Control by Gain-Scheduled Feedback with State Resets

Nobutaka Wada*,a, Member
Yi Li**, Non-member
Daichi Miyake**, Non-member
Surajet Khonjun**, Non-member

In this paper, we address the torque control problem of a permanent magnet synchronous motor (PMSM) under input voltage limitation. First, a plant model of a PMSM is derived as a linear parameter varying system in which the rotor speed is included as the varying parameter. Second, we show that setpoint tracking control is achievable under the time variation of the rotor speed. Then we show a method of constructing a control law that achieves convergence of the motor torque to a step reference signal under input voltage limitation and time variation of the rotor speed. The proposed control law consists of a gain-scheduled control law and a servo compensator. In the proposed control method, the scheduling parameter and the controller state are optimally updated so that the transient response is improved. The effectiveness of the method is shown by a numerical example.

Keywords: PMSM; tracking; saturation; integrator reset; gain-scheduling; LMIs

Received 23 January 2011; Revised 15 March 2011

1. Introduction

The permanent magnet synchronous motor (PMSM) has been widely used in various industries due to its characteristics of high efficiency, high torque to inertia ratio, and fast dynamic performance. The dynamics of the PMSM includes nonlinear coupling terms between the d-axis and q-axis subsystems. A standard approach to construct a control law for a PMSM is to use a decentralized proportional-integral (PI) controller with a decoupling compensator used to cancel the nonlinear coupling terms 1. The controller of this type is very practical since its design and implementation on the computer are fairly easy. In general, a larger control signal is required transiently to achieve higher tracking control performance, which would cause control signal saturation. When the control signal is saturated, the decoupling compensator is no longer effective. The design problem of the controller that guarantees closed-loop stability under control signal saturation is a difficult problem because of the nonlinear characteristics of the control system.

An anti-windup scheme is one way to deal with input saturation problems and has been applied to a control the problem of a PMSM in Ref. 2. It has been shown in Ref. 2 that closed-loop stability can be ensured under input voltage limitation by using an appropriately designed anti-windup compensator. However, the control law of Ref. 2 is designed under the assumption that the rotor speed is constant. Hence, the closed-loop performance would deteriorate when the rotor speed changes.

Recently, several control techniques based on optimal control theory have been applied to the control problem of a PMSM. Model predictive control schemes 3,4 have been applied to the torque control problem of a PMSM in Refs 5,6 and a velocity control problem in Ref. 7. Also, a nonlinear optimal control technique has been applied to a torque control problem of a PMSM in Ref. 8. It has been shown in above works that higher tracking control performance can be achieved under input voltage limitation as compared with the standard decentralized PI control approach. However, in these works, the controller is designed under the assumption that the rotor speed is constant. Hence, it seems that further studies are required to examine the tracking performance and stability of the control system under the variation of the rotor speed with time.

In Ref. 9, a gain-scheduled servo control law for input-constrained linear time-invariant systems was proposed. The controller in Ref. 9 consists of a servo compensator and a gain-scheduled controller. In this scheme, the scheduling parameter and the controller state are updated at each sampling time so that the tracking control performance is improved. It was shown in Ref. 10 that the optimization problem to determine the scheduling parameter and the integrator state can be solved efficiently by a simple bisection method. However, this method cannot be directly applied to the control problem of a PMSM since the method is applicable only to linear time-invariant systems.

In this paper, we develop a torque control method for a PMSM based on Ref. 9. First, a plant model of a PMSM is derived as a linear parameter varying (LPV) system in which the rotor speed is included as the varying parameter. Second, we show that setpoint tracking control is achievable under the time variation of the rotor speed. Then, we show a method of constructing a torque control law that achieves setpoint tracking under input voltage limitation and time variation of the rotor speed. To derive the control law, we extend the control law of Ref. 9 so that the LPV system can be handled. The effectiveness of the proposed method is shown by a numerical example.

Notations: For a vector $u \in \mathbb{R}^m$ and a diagonal matrix $A = [a_1, \ldots, a_m] > 0$, we define the saturation function as $\Phi_A(u) :=$

[a] Correspondence to: Nobutaka Wada. E-mail: nwada@hiroshima-u.ac.jp

* Division of Mechanical System and Applied Mechanics, Hiroshima University, 1-4-1, Kagamiyama, Higashi-Hiroshima, Hiroshima 739-8527, Japan

** Department of Mechanical Systems Engineering, Hiroshima University, 1-4-1, Kagamiyama, Higashi-Hiroshima, Hiroshima 739-8527, Japan

$(\phi_{a_1}(u_1),\ldots,\phi_{a_m}(u_m))^{\mathrm{T}}$, where

$$\phi_{a_i}(u_i) := \begin{cases} a_i \mathrm{sgn}(u_i), & |u_i| > a_i \\ u_i, & |u_i| \le a_i \end{cases}$$

If $A = I$, we will omit it. For a positive definite matrix $P \in \mathbb{R}^{n\times n}$, a vector $v \in \mathbb{R}^n$, and a positive scalar η, we define $\mathcal{E}(P,\eta,v) := \{x \in \mathbb{R}^n : (x-v)^{\mathrm{T}}P(x-v) \le \eta\}$. For a matrix $F \in \mathbb{R}^{m\times n}$, we define $\mathcal{L}(F) := \{x \in \mathbb{R}^n : |F^{(i)}x| \le 1, i = 1,\ldots,m\}$, where $F^{(i)}$ denotes the ith row of F. For integers k_1 and k_2 such that $k_1 \le k_2$, we define $I[k_1,k_2] := [k_1, k_1+1,\ldots,k_2]$. Let $\mathcal{V}$ be the set of $m \times m$ diagonal matrices whose diagonal elements are either 1 or 0. There are 2^m elements in $\mathcal{V}$. Suppose that each element of $\mathcal{V}$ is labeled as $\mathbf{E}_j, j = 1,2,\ldots,2^m$. Also, we define $\tilde{\mathbf{E}}_j := I - \mathbf{E}_j$.

2. Problem Formulation and Preliminaries

The PMSM is composed of a permanent magnet rotor and stator windings. The PMSM stator has three coils spatially separated by 120°. A rotating magnetic field is generated by the three-phase current, and the magnetic torque is generated by the interaction of the rotating magnetic field and the flux of the permanent magnet 6. In the control system design for PMSMs, the d-q rotating frame is commonly used, since AC signals appear as DC signals in the d-q rotating frame. Figure 1 shows the relationship between the d-q rotating frame and the u-v-w reference frame. In this figure, θ is the angular position of the rotor, and p is the number of pole pairs. The dynamics of a PMSM in the d-q rotating frame is described by the following differential equations 7,11:

$$\frac{\mathrm{d}i_d}{\mathrm{d}t} = \frac{1}{L_s}(-Ri_d + L_s p\omega i_q + v_d) \tag{1}$$

$$\frac{\mathrm{d}i_q}{\mathrm{d}t} = \frac{1}{L_s}(-pL_s\omega i_d - Ri_q + v_q - \omega p\phi_{\mathrm{mg}}) \tag{2}$$

$$\frac{\mathrm{d}\omega}{\mathrm{d}t} = \frac{1}{J_s}(T_e - B_v\omega) \tag{3}$$

$$T_e = \frac{3}{2}p\phi_{\mathrm{mg}}i_q \tag{4}$$

where i_d, i_q (A) are stator currents in the d-q frame, and v_d, v_q (V) represent stator voltages in the same frame. ω (rad/s) is the rotor speed. T_e (N m) is the electric magnetic torque. L_s (H) is the stator phase winding inductance. ϕ_{mg} (Wb) denotes the flux of the permanent magnet. J_s (kg m^2) is the rotor moment of inertia. B_v (N/rad/s) is the viscous coefficient. R (Ω) denotes the stator resistance.

In this paper, we consider the torque control problem of a PMSM. Hence, we choose $y = T_e$ as the controlled output. Also, the dynamical system described by (1) (2) is used for control system design. More specifically, the following discretized model of the dynamical system (1), (2) with the Euler method is used as the plant model for control system design.

$$x_p(t+1) = A_p(\omega(t))x_p(t) + B_p(v(t) - h(\omega(t))) \tag{5}$$

$$y(t) = C_p x_p(t) \tag{6}$$

where T_s (s) is the sampling period, $x_p := [i_d, i_q]^{\mathrm{T}}$ is the plant state, $v := [v_d, v_q]^{\mathrm{T}}$ is the control input, and

$$A_p(\omega) := I + T_s\begin{bmatrix} -\frac{R}{L_s} & p\omega \\ -p\omega & -\frac{R}{L_s} \end{bmatrix},\ B_p := T_s\begin{bmatrix} \frac{1}{L_s} & 0 \\ 0 & \frac{1}{L_s} \end{bmatrix},$$

$$C_p := \begin{bmatrix} 0 & \frac{3p\phi_{\mathrm{mg}}}{2} \end{bmatrix},\ h(\omega) := \begin{bmatrix} 0 \\ p\phi_{\mathrm{mg}}\omega \end{bmatrix}$$

In PMSMs, the norm constraint described by $v_d^2 + v_q^2 \le V_{\max}^2$, where $V_{\max} := V_{\mathrm{dc}}/\sqrt{3}$, is usually imposed on the input voltage 8.

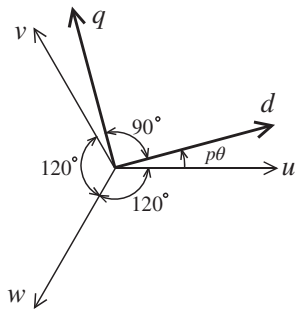

Fig. 1. Relationship between the d-q rotating frame and the u-v-w reference frame

To satisfy the constraint, we compute the input voltage by

$$v(t) = \Phi_{\overline{V}}(u(t)) \tag{7}$$

where $u \in \mathbb{R}^2$ is a new control signal. Also, $\overline{V}$ and $v_{\max}$ are defined by $\overline{V} := v_{\max}I$ and $v_{\max} := V_{\max}/\sqrt{2}$, respectively.

For the system (5), (6), we make the following assumption.

Assumption 1 *ω satisfies $\omega(t) \in [\underline{\omega}, \overline{\omega}], \forall t \ge 0$, where $\underline{\omega}$ and $\overline{\omega}$ are constants such that $\underline{\omega} \le \overline{\omega}$.*

Note that, in this case, the matrix $A_p(\omega)$ can be represented as $A_p(\omega) = \sum_{s=1}^{2}\beta_s(\omega)A_{ps}$, where $A_{p1} := A_p(\underline{\omega})$, $A_{p2} := A_p(\overline{\omega})$, $\beta_1, \beta_2 \ge 0$, and $\beta_1 + \beta_2 = 1$.

In this paper, we consider the following problem:

Problem 1 *Consider the system (5)–(7). Assume that $\omega(t) \in [\underline{\omega}, \overline{\omega}], \forall t \ge 0$. Design a control law $u(t) = \mathcal{K}(x_p(t), \omega(t), r(t))$ that ensures closed-loop stability and achieves $\lim_{t\to\infty} y(t) = r(t)$, where $r(t) = \overline{r}, \forall t \ge 0$ and $\overline{r}$ is a constant.*

In this paper, we compute the signal $u(t)$ by

$$u(t) = \tilde{v}(t) + h(\omega(t)) \tag{8}$$

where $\tilde{v} \in \mathbb{R}^2$ is a new control signal. The system (5)–(8) is expressed as

$$x_p(t+1) = A_p(\omega(t))x_p(t) + B_p[(\Phi_{\overline{V}}(\tilde{v}(t) + h(\omega(t))) - h(\omega(t))] \tag{9}$$

3. Controller Design

In this paper, we design a controller described by

$$x_c(t+1) = x_c(t) + e(t), \tag{10}$$

$$e(t) = r(t) - y(t), \tag{11}$$

$$\tilde{v}(t) = F_c(t)x_c(t) + F_p(t)x_p(t) + M(t)r(t) \tag{12}$$

where $x_c \in \mathbb{R}$ is the integrator state. The design condition of the matrices $F_c(t)$, $F_p(t)$, and $M(t)$ will be introduced later in this section. In the proposed control method, by suitably resetting the controller state x_c, we attempt to improve tracking control performance. The details of the control algorithm will be explained in Section 4.

From (9)–(11), an augmented system is derived as

$$x(t+1) = A(\omega(t))x(t) + B[\Phi_{\overline{V}}(\tilde{v}(t) + h(\omega(t))) - h(\omega(t))] + Er(t) \tag{13}$$

$$e(t) = Cx(t) + D_w r(t) \tag{14}$$

where $x := [x_p^{\mathrm{T}}, x_c]^{\mathrm{T}}$ and

$$A(\omega) := \begin{bmatrix} A_p(\omega) & 0 \\ -C_p & I \end{bmatrix},\ B := \begin{bmatrix} B_p \\ 0 \end{bmatrix},\ E := \begin{bmatrix} 0 \\ I \end{bmatrix},$$
$$C := \begin{bmatrix} -C_p & 0 \end{bmatrix},\ D_w := I$$

We also define the following matrices:

$$A_s := \begin{bmatrix} A_{ps} & 0 \\ -C_p & I \end{bmatrix},\ s = 1, 2$$

Note that $A(\omega)$ can be expressed as $A(\omega) = \sum_{s=1}^{2} \beta_s(\omega) A_s$.

The following result holds:

Lemma 1 *There exist matrices* Π *and* $\Gamma(\omega)$ *that satisfy*

$$\Pi = A(\omega)\Pi + B\Gamma(\omega) + E,\ \forall\omega \tag{15}$$
$$0 = C\Pi + D_w \tag{16}$$

Proof The solution to (15), (16) are given as

$$\Pi = \begin{bmatrix} c_1 \\ \frac{2}{3p\phi_{\mathrm{mg}}} \\ c_2 \end{bmatrix},\ \Gamma(\omega) = \begin{bmatrix} c_1 R - \frac{2L_s}{3\phi_{\mathrm{mg}}}\omega \\ \frac{2R}{3p\phi_{\mathrm{mg}}} + c_1 p L_s \omega \end{bmatrix} \tag{17}$$

where c_1 and c_2 are arbitrary constants. **Q.E.D.**

Remark 1 *Equations (15), (16) could be viewed as an extension of the regulator equation 12,13 to a class of LPV systems.*

We define the following variables.

$$\tilde{v}_e := \tilde{v} - \Gamma(\omega) r \tag{18}$$
$$\xi := x - \Pi r \tag{19}$$

From (13)–(19), the error system can be derived as

$$\xi(t+1) = A(\omega(t))\xi(t) + B[\Phi_{\overline{V}}(\tilde{v}_e(t) + \Gamma(\omega(t))r(t), \\ +h(\omega(t))) - (\Gamma(\omega(t))r(t) + h(\omega(t)))] \tag{20}$$

Remark 2 Πr *in (19) represents the steady-state value of the state* x *when the plant output* y *tracks the step reference signal* r*. Similarly,* $\Gamma(\omega)r$ *in (18) represents the steady-state value of the signal* $\tilde{v}$*. It should be noted that the solution matrix* Π *to (15), (16) is constant. This is a crucial property of the PMSM dynamics. This implies that the steady-state value of the state does not depend on the varying parameter* ω*. Note that, thanks to this property, the error system (20) can be derived. Further, this property will enable us to design a control law that achieves setpoint tracking under the time variation of the rotor speed* ω*.*

Remark 3 *In general, the steady-state value of the state of LPV systems changes depending on varying parameters. Hence, setpoint tracking is usually achievable only in the case where the varying parameter becomes constant.*

We make the following assumption:

Assumption 2 *The reference signal satisfies* $|\Gamma^{(l)}(\omega)\overline{r} + h^{(l)}(\omega)| < v_{\max},\ \forall\omega \in [\underline{\omega}, \overline{\omega}],\ l = 1, 2.$

The above assumption ensures that the tracking control is achievable under the input limitation in the steady state.

In the following, we introduce a polytopic model of a saturation function proposed in Ref. 14. The following polytopic model will be used to design the feedback controller (10)–(12).

Lemma 2 *14 Let* $u, v \in \mathbb{R}^m$*. Suppose that* $|v_j| \le 1$ *for all* $j \in I[1, m]$*; then*

$$\Phi_A(u) \in co\{\mathbf{E}_j u + \tilde{\mathbf{E}}_j v : j \in I[1, 2^m]\} \tag{21}$$

where co denotes the convex hull.

From the above lemma, it can easily be verified that, for $A = \mathrm{diag}[a_1, \ldots, a_m] > 0$ and $|v_j| \le a_j$, $\Phi_A(u)$ can be expressed as

$$\Phi_A(u) = \sum_{j=1}^{2^m} \lambda_j (\mathbf{E}_j u + \tilde{\mathbf{E}}_j v) \tag{22}$$

where $0 \le \lambda_j \le 1,\ \sum_{j=1}^{2^m} \lambda_j = 1$.

In the following, we introduce a theorem that is used to design the feedback control law (10)–(12). The control law designed on the basis of the following theorem has a structure such that a high-gain control law and a low-gain control law are interpolated by a single scheduling parameter. The scheduling parameter will be used to tune the tradeoff between the size of the region of attraction and tracking performance. The control algorithm will be introduced in Section 4.

Theorem 1 *Consider the system (13) and (14). Suppose that* $\overline{r}$ *satisfies* $\max_{\omega\in[\underline{\omega},\overline{\omega}]} |\Gamma^{(l)}\overline{r} + h(\omega)^{(l)}| < v_{\max},\ l = 1, 2$*. For given positive definite matrices* $\mathbf{R}$, $\mathbf{S}$*, positive scalars* η*,* γ_0 *and* γ_1 *such that* $\gamma_0 \le \gamma_1$*, assume that there exist matrices* $Q_i, Y_i, Z_i, (i = 0, 1)$ *that satisfy*

$$\begin{bmatrix} Q_i & * & * \\ \begin{bmatrix} \mathbf{R}^{1/2} Y_i \\ \mathbf{S}^{1/2} Q_i \end{bmatrix} & \gamma_i I & * \\ A_s Q_i + B(\mathbf{E}_j Y_i + \tilde{\mathbf{E}}_j Z_i) & 0 & Q_i \end{bmatrix} > 0, \\ \forall i \in I[0, 1],\ \forall j \in I[1, 4],\ s \in I[1, 2] \tag{23}$$

$$\begin{bmatrix} Q_i & * \\ Z_i^{(l)} & \frac{\rho_l^2}{\eta} \end{bmatrix} \ge 0, \forall i \in I[0, 1],\ \forall l \in I[1, 2], \tag{24}$$

$$Q_0 < Q_1 \tag{25}$$

where $\rho_l := v_{\max} - \max_{\omega\in[\underline{\omega},\overline{\omega}]} |\Gamma(\omega)^{(l)}\overline{r} + h(\omega)^{(l)}|$ *and the symbol* $*$ *stands for symmetric block in matrix inequalities. Further, for some constant* $\alpha \in [0, 1]$*, we suppose that* $\xi(0) \in \mathcal{E}(P(\alpha), \eta, 0)$*, where* $P(\alpha) := Q(\alpha)^{-1}, Q(\alpha) := (1-\alpha)Q_0 + \alpha Q_1$*. Then, by applying the control law*

$$\tilde{v}(t) = F(\alpha)x(t) + M(\alpha, \omega(t))r(t) \tag{26}$$

where $F(\alpha) := Y(\alpha)Q(\alpha)^{-1}$, $Y(\alpha) := (1-\alpha)Y_0 + \alpha Y_1$*, and* $M(\alpha, \omega) := \Gamma(\omega) - F(\alpha)\Pi$*, to the system (13) and (14), the relations* $\xi(t) \in \mathcal{E}(P(\alpha), \eta, 0), \forall t \ge 0$*,* $\lim_{t\to\infty} e(t) = 0$ *hold. Further,* $J := \sum_{t=0}^{\infty}\{\xi(t)^{\mathrm{T}}\mathbf{S}\xi(t) + \tilde{v}_e(t)^{\mathrm{T}}\mathbf{R}\tilde{v}_e(t)\} < \gamma(\alpha)\eta$ *holds, where* $\gamma(\alpha) := (1-\alpha)\gamma_0 + \alpha\gamma_1$*.*

Proof From (18), (19), and (26), we obtain $\tilde{v}_e = F(\alpha)\xi$. Hence, the closed-loop system (20), (26) can be represented as

$$\xi(t+1) = A(\omega(t))\xi(t) + B\Psi_{\overline{V}}(F(\alpha)\xi(t)) \tag{27}$$

where $\Psi_{\overline{V}}(F(\alpha)\xi) := \Phi_{\overline{V}}(F(\alpha)\xi + \Gamma(\omega)\overline{r} + h(\omega)) - (\Gamma(\omega)\overline{r} + h(\omega))$. We define $H(\alpha) := Z(\alpha)Q(\alpha)^{-1}$, $Z(\alpha) := (1-\alpha)Z_0 + \alpha Z_1$ and $\rho := \mathrm{diag}[\rho_1, \rho_2]$. If $\xi \in \mathcal{L}(H(\alpha), \rho)$ and $\max_{\omega\in[\underline{\omega},\overline{\omega}]} |\Gamma(\omega)^{(l)}\overline{r} + h(\omega)^{(l)}| < v_{\max},\ \forall l \in I[1, 2]$, then $|H(\alpha)^{(l)}\xi + \Gamma(\omega)^{(l)}\overline{r} + h(\omega)^{(l)}| \le v_{\max},\ \forall l \in I[1, 2],\ \forall\omega \in [\underline{\omega}, \overline{\omega}]$. Hence, in this case, the relation $\Phi(F(\alpha)\xi + \Gamma(\omega)\overline{r} + h(\omega)^{(l)}) = \sum_{j=1}^{4} \lambda_j \{\mathbf{E}_j(F(\alpha)\xi + \Gamma(\omega)r + h(\omega)) + \tilde{\mathbf{E}}_j(H(\alpha)\xi + \Gamma(\omega)\overline{r} + h(\omega))\}$ holds from Lemma 2. Therefore, the relation $\Psi_{\overline{V}}(F(\alpha)\xi) = \sum_{j=1}^{4} \lambda_j \{\mathbf{E}_j F(\alpha) + \tilde{\mathbf{E}}_j H(\alpha)\}\xi$ holds.

By using this relation, if $\xi(t) \in \mathcal{L}(H(\alpha), \rho)$ and $\max_{\omega\in[\underline{\omega},\overline{\omega}]} |\Gamma(\omega)^{(l)}\overline{r} + h(\omega)^{(l)}| < v_{\max},\ \forall l \in I[1, 2]$, the closed-loop system (27) can be rewritten as

$$\xi(t+1) = \mathcal{A}(\lambda(t), \omega(t))\xi(t) \tag{28}$$

where $\mathcal{A}(\lambda, \omega) := \sum_{j=1}^{4} \lambda_j \mathcal{A}_j(\omega),\ \mathcal{A}_j(\omega) := A(\omega) + B\{\mathbf{E}_j F(\alpha) + \tilde{\mathbf{E}}_j H(\alpha)\}$.

On the other hand, from (14) and (16), the signal $e(t)$ can be expressed as

$$e(t) = C\xi(t) \tag{29}$$

From (24), we have

$$\begin{bmatrix} Q(\alpha) & * \\ Z(\alpha)^{(l)} & \frac{\rho_l^2}{\eta} \end{bmatrix} \geq 0, \ \forall l \in I[1,2] \tag{30}$$

Then, by substituting $Z(\alpha)^{(l)} = H(\alpha)^{(l)}Q(\alpha)$ for (30) and performing a congruence transformation with block- diag$[Q(\alpha)^{-1}, 1]$ and substituting $Q(\alpha)^{-1} = P(\alpha)$, and applying Schur complement 15, we have

$$\frac{1}{\rho_l^2}H(\alpha)^{(l)T}H(\alpha)^{(l)} \leq \frac{1}{\eta}P(\alpha), \ \forall l \in I[1,2] \tag{31}$$

Equation (31) implies that $\mathcal{E}(P(\alpha), \eta, 0) \subseteq \mathcal{L}(H(\alpha), \rho)$.

By carrying out the similar procedures used to derive (30)– (23), and substituting $Z(\alpha) = H(\alpha)Q(\alpha)$ and $Y(\alpha) = F(\alpha)Q(\alpha)$ for the resulting inequality, and performing a congruence transformation with block-diag$[Q(\alpha)^{-1}, I, I]$, and multiplying the resulting inequality by $\beta_s(\omega(t))$, and summing them up for $s = 1, 2$, we have

$$\begin{bmatrix} P(\alpha) & * & * \\ \begin{bmatrix} \mathbf{R}^{1/2}F(\alpha) \\ \mathbf{S}^{1/2} \end{bmatrix} & \gamma(\alpha)I & * \\ \mathcal{A}_j(\omega(t)) & 0 & P(\alpha)^{-1} \end{bmatrix} > 0 \tag{32}$$

Further, by multiplying the inequality (32) by $\lambda_j(t)$, and summing them up for $j = 1, \ldots, 4$, we have

$$\begin{bmatrix} P(\alpha) & * & * \\ \begin{bmatrix} \mathbf{R}^{1/2}F(\alpha) \\ \mathbf{S}^{1/2} \end{bmatrix} & \gamma(\alpha)I & * \\ \mathcal{A}(\lambda(t), \omega(t)) & 0 & P(\alpha)^{-1} \end{bmatrix} > 0 \tag{33}$$

By applying Schur complement to (33), and multiplying the resulting inequality from the left by $\xi(t)^{\mathrm{T}}$ and from the right by $\xi(t)$, and using (28) and (29), we have

$$\begin{aligned} & V(\xi(t+1)) - V(\xi(t)) \\ < & -\frac{1}{\gamma(\alpha)}\{\xi(t)^{\mathrm{T}}\mathbf{S}\xi(t) + \tilde{v}_e(t)^{\mathrm{T}}\mathbf{R}\tilde{v}_e(t)\} \end{aligned} \tag{34}$$

where $V(\xi) := \xi^{\mathrm{T}}P(\alpha)\xi$. From (34), we can conclude that, if $\xi(0) \in \mathcal{E}(P(\alpha), \eta, 0)$, then

$$V(\xi(t)) < V(\xi(0)) \leq \eta, \quad \forall t \geq 0 \tag{35}$$

Equation (35) implies that $\xi(t) \in \mathcal{E}(P(\alpha), \eta, 0), \ \forall t \geq 0$. On the other hand, it has been shown that the nonlinearity $\Psi(F(\alpha)\xi(t))$ can be represented as $\Psi(F(\alpha)\xi(t)) = \sum_{j=1}^{4}\lambda_j(t)\{\mathbf{E}_j F(\alpha) + \tilde{\mathbf{E}}_j H(\alpha)\}\xi(t)$ if $\xi(t) \in \mathcal{L}(H(\alpha), \rho)$ and $\max_{\omega\in[\underline{\omega},\overline{\omega}]} |\Gamma^{(l)}\overline{r} + h(\omega)^{(l)}| < v_{\max}, \ \forall l \in I[1,2]$. From (31) and (35), we can state that, if the conditions in Theorem 1 hold, the relation $\xi(t) \in \mathcal{L}(H(\alpha), \rho), \ \forall t \geq 0$ holds. From (34), since $\xi(t) \to 0, (t \to \infty)$, $e(t) \to 0, (t \to \infty)$ holds. Moreover, from (34) and (35), $J = \sum_{t=0}^{\infty}\{\xi(t)^{\mathrm{T}}\mathbf{S}\xi(t) + \tilde{v}_e(t)^{\mathrm{T}}\mathbf{R}\tilde{v}_e(t)\} < \gamma(\alpha)\eta$ holds. **Q.E.D**.

Based on Theorem 1, we design a gain $F(1) = Y_1Q_1^{-1}$, which makes the region $\mathcal{E}(P(1), \eta, 0)$ large, and a gain $F(0) = Y_0Q_0^{-1}$, which achieves fast convergence of the state in $\mathcal{E}(P(0), \eta, 0)$, by suitably choosing the parameters γ_0, γ_1, $\mathbf{R}$, and $\mathbf{S}$. Then we construct the control law (26) by interpolating the obtained gains.

Remark 4 *When the control law (26) is designed based on Theorem 1, the matrix $P(\alpha)$ needs to be determined so that the condition $\xi(0) \in \mathcal{E}(P(\alpha), \eta, 0)$ is satisfied for some constant $\alpha \in [0, 1]$. This can be achieved by solving the design problem with the constraint $\xi(0) \in \mathcal{E}(P_1, \eta, 0)$. By applying the Schur complement, this condition can be rewritten as the following linear matrix inequality (LMI) condition:*

$$\begin{bmatrix} \eta & * \\ x(0) - \Pi\overline{r} & Q_1 \end{bmatrix} \geq 0 \tag{36}$$

Also, the conditions (23)–(25) are LMIs with respect to the variables $Q_i, Y_i, Z_i, (i = 0, 1)$. Hence, the design problem of the control law (26) that satisfies (23)–(25) and (36) can be solved efficiently by a numerical optimization algorithm based on an interior point method 15.

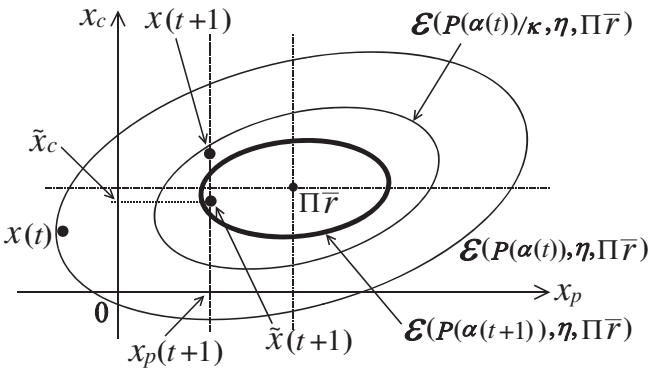

Fig. 2. Graphical interpretation of the optimization problem at Step 3 in Algorithm 1. In this figure, the controller state x_c is reset so that $\alpha(t+1)$ is minimized at time $t+1$. As the result, the state at time $t+1$ is moved from $x(t+1)$ to $\tilde{x}(t+1)$

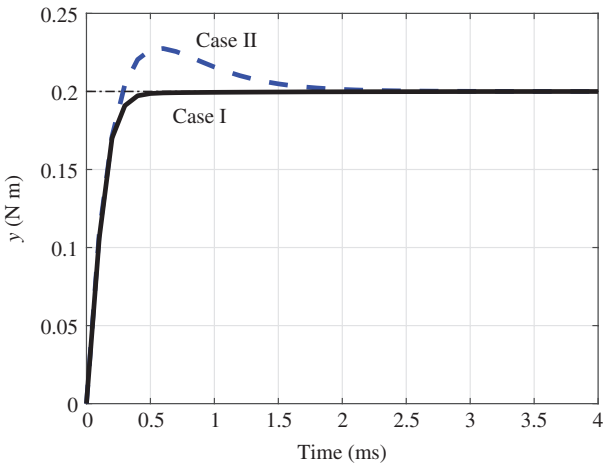

Fig. 3. Plant output y (N m)

Remark 5 *The size of the set $\mathcal{E}(P_1, \eta, 0)$ mainly depends on the choice of the parameter γ_1. By choosing a larger value as γ_1, the size of the set $\mathcal{E}(P_1, \eta, 0)$ could be expanded in general. However, the control law designed based on Theorem 1 can only ensure local stability. This implies that, when the magnitude of the reference signal $\overline{r}$ is large, there may not exist a solution that satisfies the conditions (23)–(25) and (36) even if a large value is chosen for γ_1.*

Remark 6 *If $A = A_s, \forall s \in I[1,2]$ and $h(\omega) = 0, \forall\omega \in [\underline{\omega}, \overline{\omega}]$, Theorem 1 is equivalent to Theorem 1 of Ref. 9.*

4. Control Algorithm

The control law (26) includes the scalar α. The upper bound of the cost function J is given as $\gamma(\alpha)\eta$, and the function $\gamma(\alpha)$ takes a

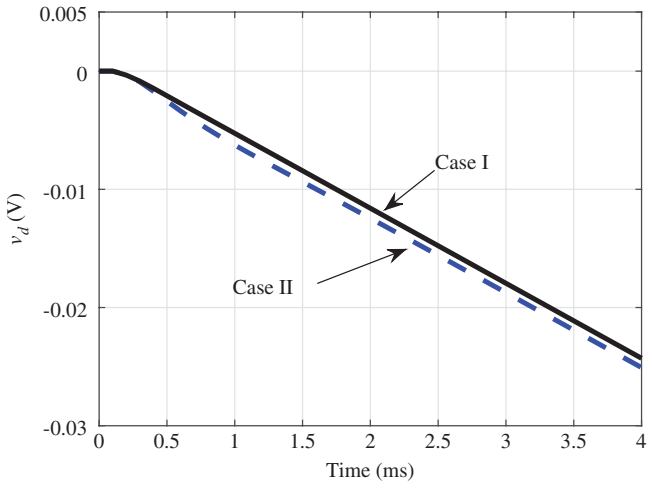

Fig. 4. d-Axis voltage v_d (V)

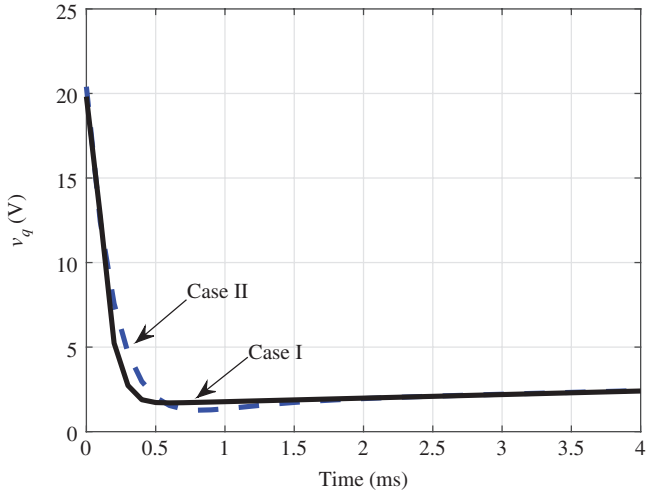

Fig. 5. q-Axis voltage v_q (V)

smaller value when a smaller value is chosen as α. Hence, it can be expected that the control performance is improved by minimizing α at each sampling time. Moreover, the state of the controller x_c can be used as a tuning parameter to improve the control performance. Thus, we utilize the following control algorithm:

Algorithm 1
Step 0: Set $t = 0$ *and* $\alpha = 1$.
Step 1: Measure $x_p(t)$ *and* $y(t)$.
Step 2: If $\alpha = 0$, *set* $\alpha(t) = 0$ *and go to Step 4.*
Step 3: For given $x_p(t)$, *solve* $\min_{\alpha\in[0,1],\ \tilde{x}_c\in\mathbb{R}} \alpha$, *s.t.*

$$\begin{bmatrix} \eta & * \\ \begin{bmatrix} x_p(t) \\ \tilde{x}_c \end{bmatrix} - \Pi\overline{r} & Q(\alpha) \end{bmatrix} > 0 \tag{37}$$

Then, set $\alpha(t) = \alpha$ *and* $x_c(t) = \tilde{x}_c$.
Step 4: Apply $v(t) = \Phi_{\overline{V}}(F(\alpha(t))[x_p(t)^{\mathrm{T}}, x_c(t)]^{\mathrm{T}} + M(\alpha(t), \omega(t))r(t) + h(\omega(t)))$ *to the plant (5), (6).*
Step 5: Compute $x_c(t+1)$ *by (10) and (11).*
Step 6: $t \leftarrow t+1$ *and go to Step 1.*

It should be noted that the value of the controller state x_c is reset so that the scheduling parameter α is minimized at Step 3 at each sampling time.

Remark 7 *The optimization problem of Step 3 in Algorithm 1 is an LMI optimization problem with respect to* α *and* $\tilde{x}_c$. *It has been shown in Ref. 10 that the optimization problem can be solved efficiently by a simple bisection algorithm.*

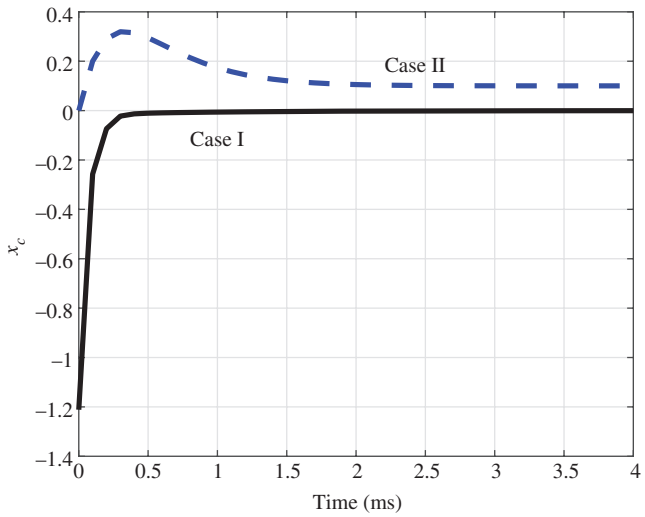

Fig. 6. Integrator state x_c

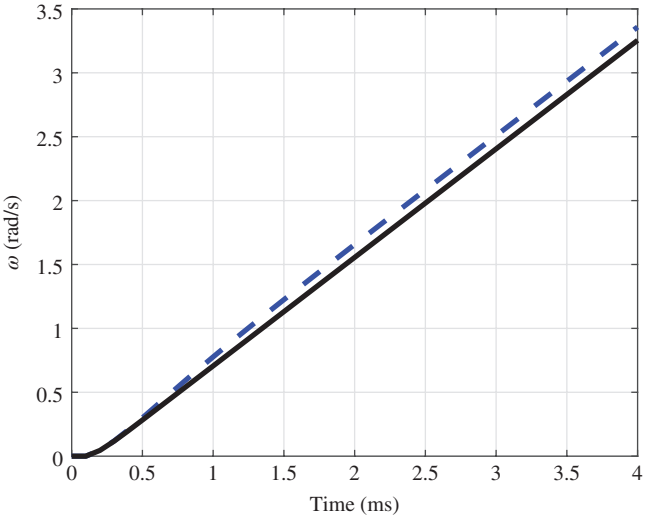

Fig. 7. Rotor speed ω (rad/s)

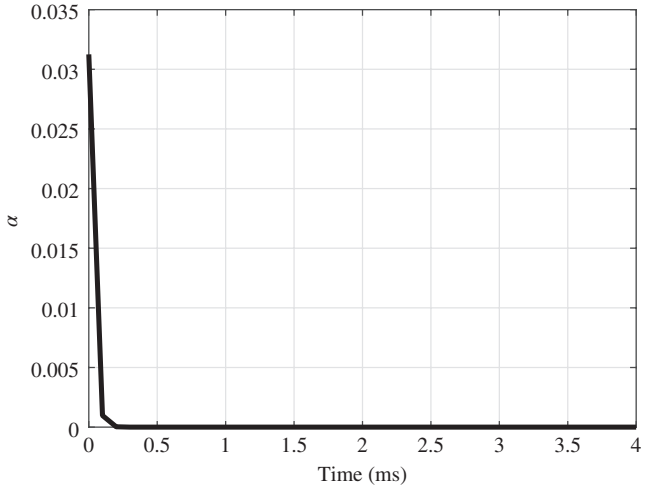

Fig. 8. Scheduling parameter α

Remark 8 *Algorithm 1 is equivalent to the control algorithm in Ref. 9 except for the structure of the control law at Step 4.*

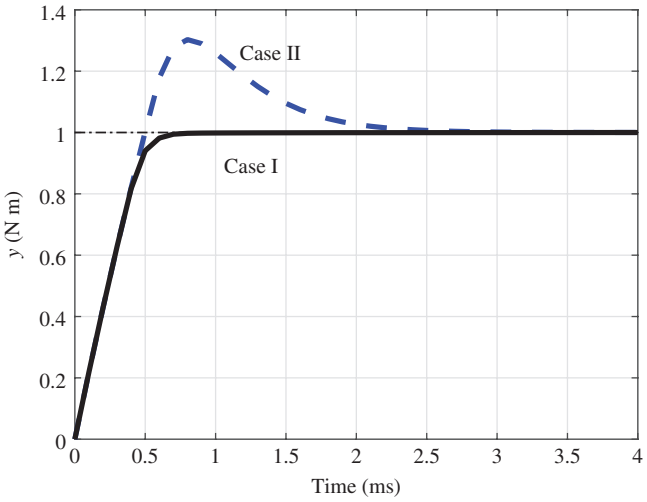

Fig. 9. Plant output y (N m)

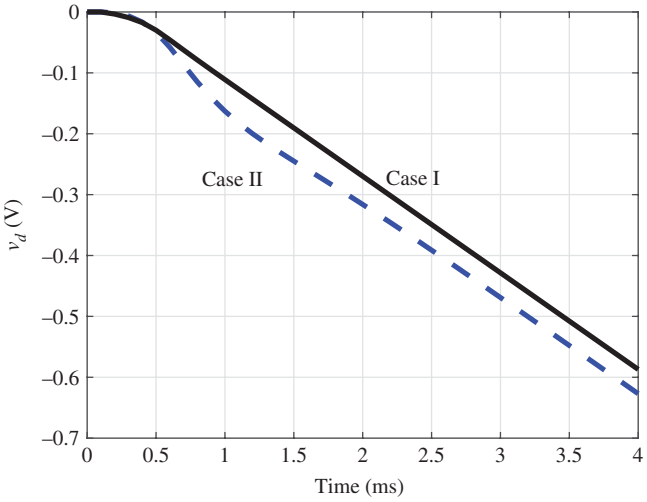

Fig. 10. d-Axis voltage v_d (V)

As for feasibility of Algorithm 1 and closed-loop stability, the following result holds:

Theorem 2 *Consider the system (5), (6). Assume that* $\omega(t)$ *satisfies* $|\Gamma(\omega(t))^{(l)}\overline{r} + h(\omega(t))^{(l)}| < v_{\max}, \forall l \in I[1,2], \forall t \geq 0$. *Moreover, assume that there exists* $\tilde{x}_c$ *such that* $[x_p(0)^{\mathrm{T}}, \tilde{x}_c]^{\mathrm{T}} \in \mathcal{E}(P(1), \eta, \Pi\overline{r})$. *Then by applying Algorithm 1 to the system (5), (6),* $e(t)$ *converges to zero as* $t \to \infty$.

Theorem 2 is a slightly modified version of Theorem 2 of Ref. 9 and can be readily proven by using the proof procedure of Ref. 9. Hence, we omit the details of the proof of Theorem 2 and outline the proof briefly. We assume that $x(t) \in \mathcal{E}(P(\alpha(t)), \eta, \Pi\overline{r})$ holds at time t, as shown in Fig. 2. When the control signal $v(t) = \Phi_{\overline{V}}(F(\alpha(t))[x_p(t)^{\mathrm{T}}, x_c(t)]^{\mathrm{T}} + M(\alpha(t), \omega(t))r(t) + h(\omega(t)))$ is applied to the system (5), (6), $[x(t) - \Pi\overline{r}]^{\mathrm{T}}P(\alpha(t))[x(t) - \Pi\overline{r}] > [x(t+1) - \Pi\overline{r}]^{\mathrm{T}}P(\alpha(t))$ $[x(t+1) - \Pi\overline{r}]$ holds from Theorem 1. Hence, for some positive scalar $\kappa < 1$, $x(t+1) \in \mathcal{E}(P(\alpha(t))/\kappa, \eta, \Pi\overline{r})$ holds. This implies that there exists $\alpha(t+1)$ such that $x(t+1) \in \mathcal{E}(P(\alpha(t+1)), \eta, \Pi\overline{r})$ and $\alpha(t+1) < \alpha(t)$. Hence, the scheduling parameter $\alpha(t)$ decreases monotonically and converges to zero. Note that the convergence speed of the parameter $\alpha(t)$ could be enhanced by resetting the integrator state x_c at each sampling time (see Fig. 2). After $\alpha(t)$ becomes zero, the constant high-gain feedback control law with the integral action is applied to the system. As the result, the tracking error $e(t)$ converges to zero.

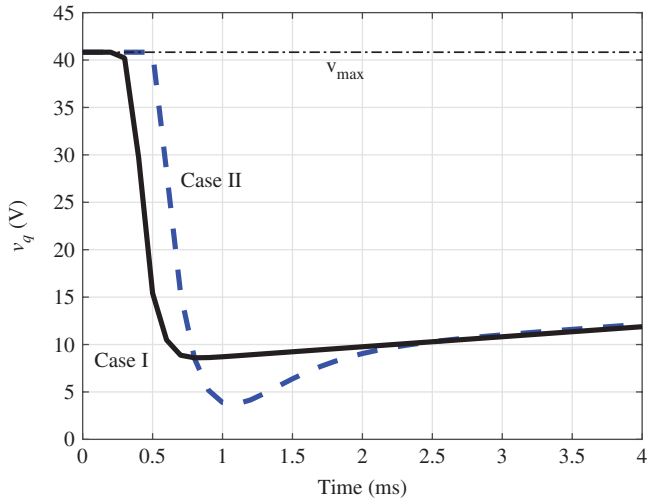

Fig. 11. q-Axis voltage v_q (V)

5. Comparison with an Existing Method

A standard approach to constructing a control law for the PMSM is to use a decentralized PI controller with a decoupling compensator used to cancel the nonlinear coupling terms of the PMS dynamics 1. In this approach, first, the decoupling compensator, defined by

$$\begin{bmatrix} u_1 \\ u_2 \end{bmatrix} = \begin{bmatrix} \tilde{v}_d - L_s p \omega i_q \\ \tilde{v}_q + p L_s \omega i_d + \omega p \phi_{\mathrm{mg}} \end{bmatrix} \tag{38}$$

is applied to the system (5), (6) to cancel the nonlinear coupling terms. Then the following decentralized PI controller is used to achieve the setpoint tracking:

$$x_c(t+1) = x_c(t) + e(t) \tag{39}$$

$$e(t) = r(t) - y(t) \tag{40}$$

$$\tilde{v}_q(t) = K_P e(t) + K_I x_c(t) \tag{41}$$

$$\tilde{v}_d(t) = K_F i_d(t) \tag{42}$$

$$v(t) = \Phi_{\overline{V}}(u(t)) \tag{43}$$

where K_P, K_I and K_F are feedback gains. When the equality $v(t) = u(t)$ holds, the closed-loop system (5), (6), (38)–(43) is divided into two linear time-invariant systems. The feedback gains of the controller can be designed by solving two independent state-feedback controller design problems. In addition, the implementation of the control algorithm on the computer is fairly easy. Hence, the above control law is very practical. However, when the signal $v(t)$ is saturated, the decoupling compensator (38) is no longer effective. As a result, the closed-loop stability with the control law (38)–(43) might not be guaranteed under such a situation. The analysis of the closed-loop system is a difficult problem due to the nonlinear characteristics of the feedback system.

6. Numerical Example

The values of the physical parameters are $J_s = 2.35 \times 10^{-4}$ kg m^2, $B_v = 1.1 \times 10^{-4}$ N/rad/s, $L_s = 7 \times 10^{-3}$ H, $R = 2.98\,\Omega$, $\phi_{\mathrm{mg}} = 0.125$ Wb, $V_{\mathrm{dc}} = 100$ V ($v_{\max} = 40.82$ V), and $p = 2$. The sampling period is chosen as $T_s = 0.1$ ms. For this plant, we designed the control law (26) with $\mathbf{S} = \mathrm{diag}[0.1, 0.1, 0.01]$, $\mathbf{R} = 10^{-5}I$, $\rho = \mathrm{diag}[37.46, 10.38]$, $\gamma_1 = 60, \gamma_0 = 0.2$, $\eta = 1$, $\overline{r} = 1$ N m, $\underline{\omega} = -100$ rad/s, $\overline{\omega} = 100$ rad/s, $c_1 = 0$, and $c_2 = 0$.

- Case I: Algorithm 1 is applied.

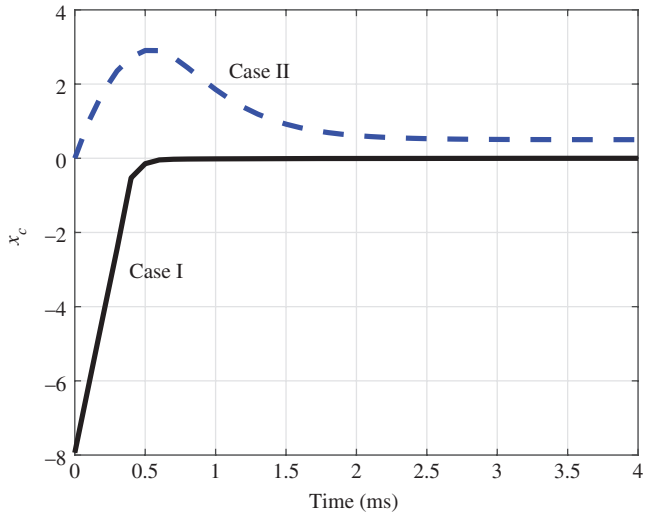

Fig. 12. Integrator state x_c

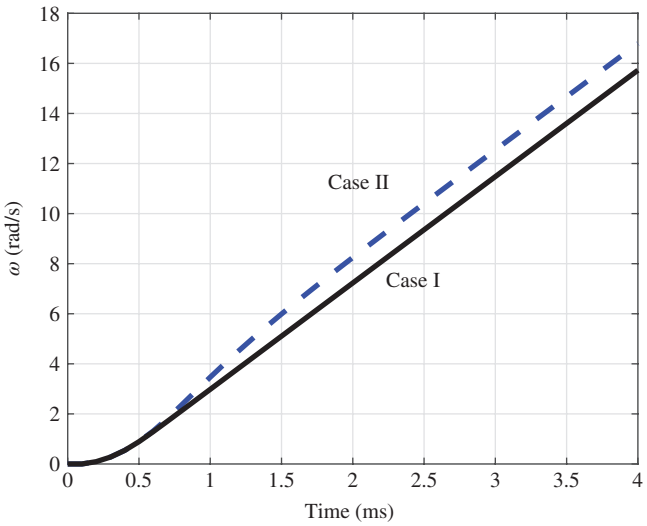

Fig. 13. Rotor speed ω (rad/s)

- Case II: Decentralized PI control with the nonlinear decoupling feedback compensation in Section 5 is applied. The feedback gains are chosen as $K_P = 111.5, K_I = 18.82, K_F = -32.02$.

Figures 3–8 show the results of the numerical simulation for the reference signal $r(t) = 0.2\,\mathrm{N\,m}$, $t \geq 0$. As the dynamical model of the PMSM to carry out the numerical simulation, we have used the discretized model of (1)–(4). The discretization was done using the Euler method with the sampling period $T_s = 0.1\,\mathrm{ms}$. The initial values of i_d, i_q, and ω were set to zero. In both cases, the maximum values of $|v_d|$ and $|v_q|$ are smaller than $v_{\max} = 40.82\,\mathrm{V}$. Further, in both cases, the controlled output y converges to the reference signal even though the rotor speed ω increases. In Case II, the controlled output tracks the reference signal with the 12.5% overshoot, and the settling time is 1.6 ms. In Case I, the controlled output tracks the reference signal without producing any overshoot, and the settling time is 0.5 ms.

Figures 9–14 show the results of the numerical simulation for the reference signal $r(t) = 1\,\mathrm{N\,m}$, $t \geq 0$. The initial values of i_d, i_q, and ω were set to zero. Note that in this numerical simulation, the signal v_q is in the saturation region transiently. In Case II, the controlled output y tracks the reference signal with the 30% overshoot, and the settling time is 2.2 ms. The larger overshoot might be due to the fact that the decoupling compensator (38) is no longer effective and the integrator windup occurs while the signal v_q is saturated. In Case I, the controlled output tracks the reference signal without producing the overshoot, and the settling

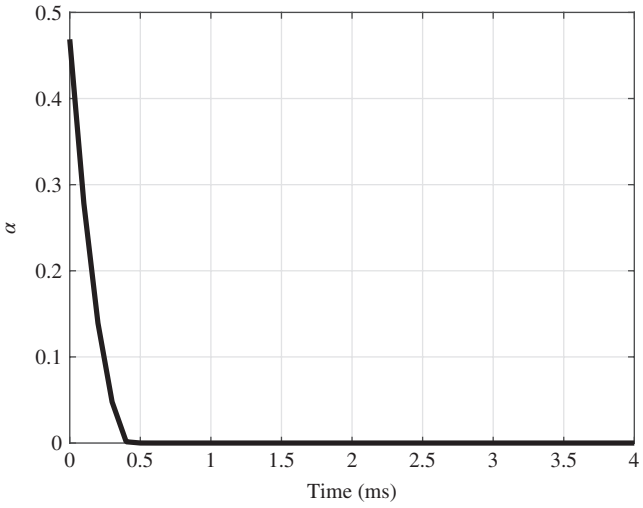

Fig. 14. Scheduling parameter α

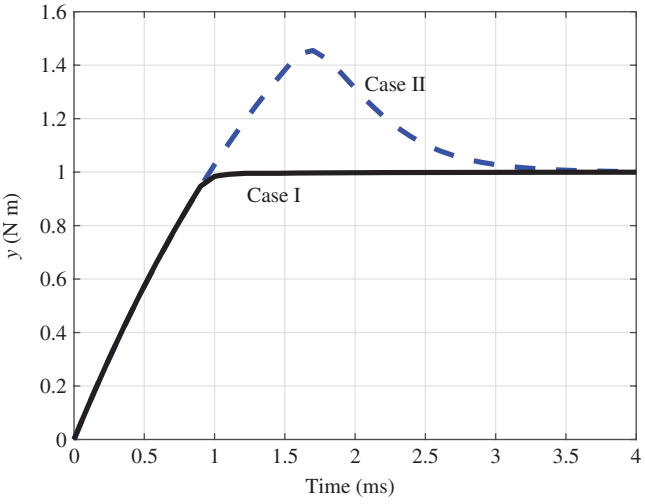

Fig. 15. Plant output y (N m)

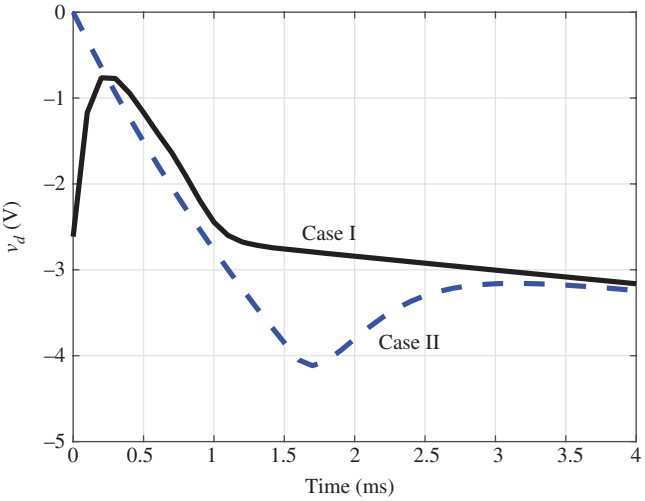

Fig. 16. d-Axis voltage v_d (V)

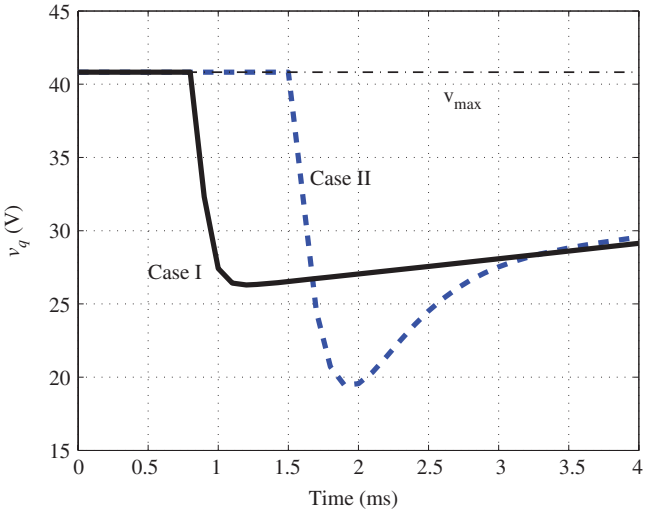

Fig. 17. q-Axis voltage v_q (V)

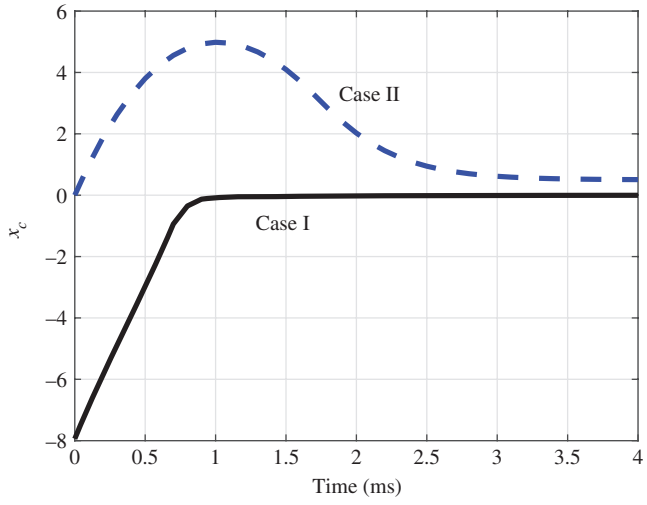

Fig. 18. Integrator state x_c

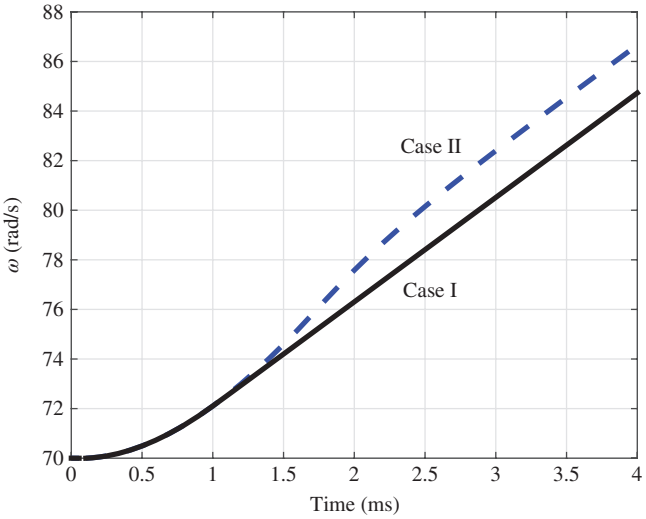

Fig. 19. Rotor speed ω (rad/s)

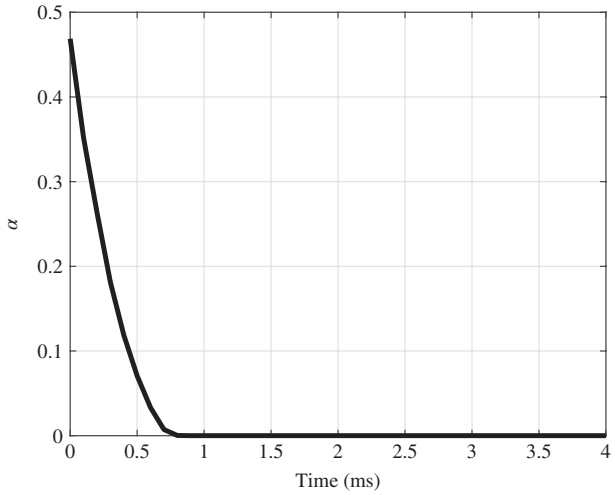

Fig. 20. Scheduling parameter α

time is 0.7 ms. In the proposed method, the integrator state x_c is reset until α becomes zero. Hence, the integrator state x_c does not accumulate while the resets are carried out. It seems that this enables the response without the overshoot.

Figures 15–20 show the results of the numerical simulation for the reference signal $r(t) = 1\,\mathrm{N\,m}$, $t \geq 0$. In this numerical simulation, the initial values of ω was set to 70 rad/s. The initial values of i_d and i_q were set to zero. It can be seen from these figures that the plant output y in Case I converges to the reference signal rapidly without producing any overshoot.

All the numerical simulations were performed with a digital computer (Intel Xeon 3.6 GHz, 4 GB RAM), using MATLAB. The maximum computation time required to solve the optimization problem in Algorithm 1 was 0.36 ms. The computation time could be reduced by using a compiled language 10.

7. Conclusions

In this paper, we have proposed a torque control method for PMSM under input voltage limitation. In the proposed control method, the scheduling parameter and the controller state are updated at each sampling time so that the tracking control performance is improved. It was shown that, by using the proposed control method, setpoint tracking is achievable under the variation of the rotor speed and the input voltage limitation. The control method in this paper is applicable only to the case where the reference signal is a step signal. Hence, it is required to extend the control method so that a time-varying reference signal can be handled. This extension could be done by introducing the target recalculation mechanism in Ref. 16 to the proposed control method. We would like to leave the extension as a future research topic.

Acknowledgments

This work was supported by the Electric Technology Research Foundation of Chugoku.

References

(1) Matsui N, Kameda K, Takeshita T. DSP-based software de-coupling current control of brushless motor. *IEEJ Transactions on Industry Applications* 1987; **107-D**(**2**):215–222 (in Japanese).
(2) March P, Turner MC. Anti-windup compensator designs for nonsalient permanent-magnet synchronous motor speed regulators. *IEEE Transactions on Industry Applications* 2009; **45**(**5**):1598–1609.
(3) Mayne DQ, Rawlings JB, Rao CV, Scokaert POM. Constrained model predictive control: stability and optimality. *Automatica* 2000; **36**:789–814.

(4) Wada N. Model predictive tracking control for constrained linear systems using integrator resets. *IEEE Transactions on Automatic Control* 2015; **60**(**11**):3113–3118.
(5) Kadota M, Doki S, Okuma S. Application of model predictive control for current control system of permanent magnet synchronous motor. *Transactions of the Institute of Electrical Engineers of Japan C* 2011; 131(**4**):860–869 (in Japanese).
(6) Zanma T, Kawasaki M, Liu K, Hagino M, Imura A. Model predictive direct torque control for PMSM with discrete voltage vectors. *IEEJ Journal of Industry Applications* 2014; **3**(**2**):121–130.
(7) Chai S, Wang L, Rogers E. Model predictive control of a permanent magnet synchronous motor with experimental validation. *Control Engineering Practice* 2013; **21**(**11**):1584–1593.
(8) Umemura Y, Sakamoto N. Nonlinear optimal servo control design for PMSM with inverter voltage norm constraints. *Transactions of the Institute of Systems, Control and Information Engineers* 2013; **26**(**7**):252–260 (in Japanese).
(9) Wada N. Constrained tracking control by continuous resets of the state of a gain-scheduled controller. *Mechanical Engineering Journal* 2014; **1**(**3**): DOI: 10.1299/mej.2014dr0012.
(10) Wada N, Miyahara H, Saeki M. Constrained tracking control by gain-scheduled feedback with optimal state resets: a general servo problem and an online optimization method. *ASME Journal of Dynamic Systems, Measurement, and Control* 2016; **138**(**12**):121008.
(11) Pillay P, Krishnan R. Modeling of permanent magnet motor drives. *IEEE Transactions on Industrial Electronics* 1988; **35**(**4**):537–541.
(12) Francis BA. The linear multivariable regulator problem. *SIAM Journal on Control and Optimization* 1975; **15**:80–505.
(13) Mantri R, Saberi A, Lin Z, Stoorvogel AA. Output regulation for linear discrete-time systems subject to input saturation. *International Journal of Robust and Nonlinear Control* 1997; **7**:1003–1021.
(14) Hu T, Lin Z, Chen BM. An analysis and design method for linear systems subject to actuator saturation and disturbance. *Automatica* 2002; **38**:351–359.
(15) Boyd S, Ghaoui LE, Feron E, Balakrishnan V. *Linear Matrix Inequalities in System and Control Theory*. SIAM: Philadelphia, PA; 1994.
(16) Wada N, Kawaoka N, Saeki M. A gain-scheduled control algorithm for input constrained systems to track time-varying references using controller state resets. *IEEJ Transactions on Electrical and Electronic Engineering* 2017; **12**(**1**):87–95.

Nobutaka Wada (Member) received the B.E., M.E., and Ph.D. degrees, all in engineering, from Hiroshima University (HU). He was an Assistant Professor with HU from 2001 to 2009, and an Associate Professor with Tottori University from 2009 to 2011. He has been an Associate Professor with HU since 2011. His research interests include constrained control, gain-scheduled control, and control application to mechanical systems. Dr Wada is a member of the SICE, ISCIE, JSME, RSJ, and IEEE.

Yi Li (Non-member) received the B.E. degree in mechanical engineering from Dalian Jiaotong University, China, in 2013. He is currently pursuing the Master's degree in the Department of Mechanical Systems Engineering, Hiroshima University. Mr Li is a member of the SICE.

Daichi Miyake (Non-member) received the B.E. degree in mechanical systems engineering from Hiroshima University (HU) in 2016. He is currently pursuing the Master's degree in the Department of Mechanical Systems Engineering, HU. Mr Miyake is a member of the SICE.

Surajet Khonjun (Non-member) received the B.E. and M.E. degrees, both in industrial engineering, from Ubon Ratchathani University (URU), Thailand, in 2004 and 2009, respectively. Currently, he is pursuing the Ph.D. degree in the Department of Mechanical Systems Engineering, Hiroshima University. Since 2005, he has been with URU, where he is currently a Lecturer.